JOURNAL OF OPTOELECTRONICS AND ADVANCED MATERIALS Vol. 24, No. 7-8, July – August 2022, p. 395 - 401

Synthesis and properties of three Ir(III) complexes using 3,6-diphenylimidazo[2,1-b]oxazole as primary ligand

X.-Q. LIU, P.-B. SI, A.-H. ZHOU, D.-Q. WANG, M.-Y. TENG*, Q. WANG*, B. LIU*

Faculty of Chemistry & Chemical Engineering, Yunnan Normal University, Kunming 650500, China

Three iridium complexes of $(dpio)_2Ir(pic)$, $(dpio)_2Ir(3\text{-}IQA)$ and $(dpio)_2Ir(2\text{-}QA)$ were synthesized efficiently by using 3,6-diphenylimidazo[2,1-b]oxazole (dpio) as primary ligands which can be prepared by facile and environmental friendly method, and 2-picolinic acid (pic), isoquinolinic acid (3-IQA) and 2-quinolinic acid (2-QA) as auxiliary ligands. Their maximum emission wavelengths are from 585 nm to 637 nm, and the luminous colors are between the yellow to red light region. The quantum efficiencies range from 14.3% to 23.8%. The results show that they have good luminous performances and are candidates as red and orange organic phosphorous materials.

(Received January 22, 2021; accepted August 10, 2022)

Keywords: Imidazolo[2,1-b]oxazole derivative, Iridium complexes, Phosphorescent materials

1. Introduction

Due to their strong spin-orbit coupling (SOC) effect caused by heavy atoms, transition metal phosphorescent complexes with d^6, d^8 and d^{10} electronic structures could make the triple excitons pass to the single-excited state through intersystem crossing (ISC), which can increase the theoretical quantum efficiency to 100%[1-3]. Among various phosphorescent materials such as complexes of Pt^{II}, Eu^{III}, Ir^{III}, etc., Ir^{III} complexes have many advantages, such as good thermal stability, relatively short excited state lifetime, high luminous efficiency, and high adjustability of luminous color, etc., which have become the research focus in the field of electroluminescent phosphorescent materials [4-15].

In 2019, we firstly reported Ir^{III} complexes with 3-methyl-6-phenyl-imidazo[2,1-b]thiazole (mpmt) as primary ligand, which can not only be facilely prepared from thiourea, acetone and acetophenone as starting materials, but also has strong coordination ability to synthesize complexes efficiently, moreover the light-emitting colors of complexes can be adjusted from red to green easily by inducting different auxiliary ligands [16]. In this paper, three novel Ir^{III} complexes using 3,6-diphenylimidazo[2,1-b]oxazole (dpio) as primary ligand which is similar in structure to mpmt, and 2-picolinic acid (pic), 3-isoquinolinic acid (3-IQA) and 2-quinolinic acid (2-QA) as auxiliary ligands were prepared. Their structures were characterized by NMR and mass spectrometry. Furthermore, the photochemical properties of these Ir^{III} complexes were investigated and analyzed basing on the different auxiliary ligands.

2. Experimental section

2.1. General information

Commercially available analytically pure reagents were used in all experiments. NMR data were measured by Bruker 500 MHz NMR spectrometer (TMS as internal standard, $CDCl_3$ or D_6-DMSO as solvents). Infrared spectra were recorded by Bruker Tensor27 infrared spectrometer. The UV-Vis absorption and fluorescence spectra were performed on Shanghai Mapoda UV-3100 UV-Vis spectrophotometer and HITACHI F-4600 spectrophotometer respectively, all samples were prepared as DMF solution at 1×10^{-5} mol·L^{-1} in a 25 mL brown volumetric flask at room temperature.

The calculation formula of the luminescence quantum efficiencies of the complexes is shown in Eq. 1:

$$\Phi_s = \Phi_{std}[I_s A_{std}/(I_{std} A_s)](\eta_s/\eta_{std})^2 \quad (1)$$

The Φ_s and Φ_{std} represent the luminescence quantum yields of the the title complexes and Ir(ppy)$_3$. I_s and I_{std} are the integrated emission intensities of the title complexes and Ir(ppy)$_3$ solution. A_{std} and A_s refer to the absorbances of the title complexes and Ir(ppy)$_3$ solution under their excitation wavelength. η_s and η_{std} are the refractive indices of the corresponding solvents (pure solvents were assumed). Ir(ppy)$_3$ was used as the internal standard and the corresponding luminescence quantum yield was 0.4 [17].

Cyclic voltammetry (CV) curves of the title complexes were measured by IM6ex (Zahner) electrochemistry working station at room temperature. Before the measurement, 3.29 mg potassium ferricyanide, 1 g potassium nitrate were dissolved into 10 mL distilled water, which was used to test whether the electrodes were in appropriate condition. Then the CV curves of title complexes were determined using 0.1 mol·L^{-1} n-Bu_4PF_6 DMF solution as supporting electrolyte, ferrocene as the internal standard with the oxidation potential of 0.42 V, using glassy carbon electrode as working electrode, Ag/Ag$^+$ electrode as reference electrode, platinum electrode as counter electrode. The scanning range was from –2 V to 1 V with scanning speed of 0.1 V·s^{-1}.

2.2. Syntheses procedure

2.2.1. Preparation of 1Chcl:2Urea DES [18]

The synthesis of the intermediate 4-phenyl-2-aminoxazole was required in the deep eutectic solvent (DES) 1CHCl :2Urea DES, as described below:

Placed 60.06 g (1 mol) urea and 69.81 g (0.5 mol) choline chloride into two 250 mL beaker, then used a vacuum drying oven to dry at 80℃ under vacuum for 48 hours. The two compounds were homogeneously mixed in a 1000 mL round bottom flask, heated and stirred to melt at 80℃. The deep eutectic solvent 1 CHCL:2 Urea DES was obtained as a colorless transparent sticky liquid.

2.2.2. Synthesis of 4-phenyl-2-aminooxazole

In a 250 mL round bottom flask, 1.20 g (20 mmol) urea and 3.98 g (20 mmol) bromide acetophenone were stirred at 80°C in a solvent of 70.0 g 1CHCL:2Urea DES for 6 hours, to give orange yellow sticky solution. After the reaction was completed, the mixture was cooled to room temperature and 40 mL water was added into the reaction mixture. The mixture was extracted by CH_2Cl_2 (40 mL × 6), organic phases was collected and dried by anhydrous $MgSO_4$. The solution was collected by suction filtration and the solvent was removed by rotary vacuum distillation. Then, the residue was purified by column chromatography (PE:EA = 2:1, volume ratio) to give pure 4-phenyl-2-aminooxazole as yellow powder.

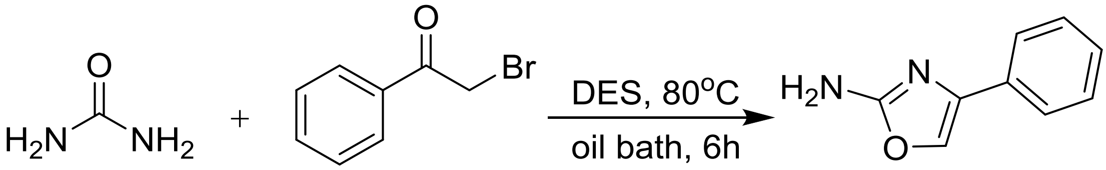

Scheme 1. Synthesis of 4-phenyl-2-aminooxazole

4-phenyl-2-aminooxazole: yellow powder, yield: 85.6 %. ^{1}H NMR (500 MHz, $CDCl_3$) δ 7.67-7.63 (m, 2H), 7.48 (s, 1H), 7.39 (t, *J* = 7.6 Hz, 3H), 7.32-7.28 (m, 2H). ^{13}C NMR (125 MHz, $CDCl_3$) δ 160.18, 140.17, 131.48, 128.60, 127.71, 127.55, 125.16. ESI-MS m/z (%)161.07 (100) [M+1]$^+$.

2.2.3. Synthesis of 3,6-diphenyl-Imidazo[2,1-b]oxazole

1.60 g (10 mmol) 4-phenyl-2-aminooxazole and 1.99 g (10 mmol) bromide acetophenone in 80 mL of anhydrous ethanol, were heated to reflux for 24 hours to get wine red reaction solution. After the mixture was cooled to room temperature, the solvent was evaporated at vacuum, the residue was purified by silica column (PE: EA = 4:1, volume ratio) pure 3,6-diphenyl-imidazo[2,1-b]oxazole was obtained as yellow powder.

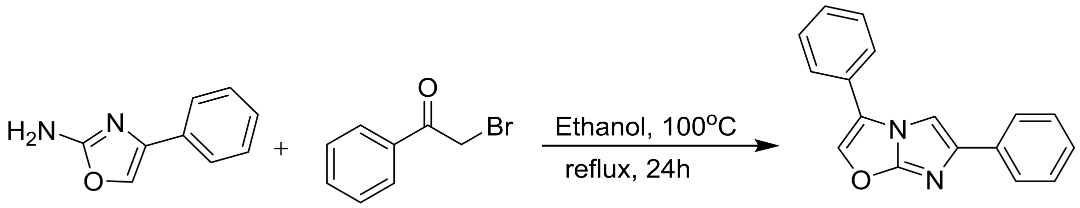

Scheme 2. Synthesis of 3,6-diphenyl-Imidazo[2,1-b]oxazole

3,6-diphenyl-imidazo[2,1-b]oxazole: yellow powder, yield: 57.8 %. ^{1}H NMR (500 MHz, Acetone) δ 8.22 (s, 1H), 8.17 (s, 1H), 7.94 (dd, J = 8.3, 1.2 Hz, 2H), 7.93-7.89 (m, 2H), 7.61 (dd, J = 10.4, 4.8 Hz, 2H), 7.53 (dd, J = 8.4, 6.5 Hz, 1H), 7.40 (t, J = 7.7 Hz, 2H), 7.27 (t, J = 7.4 Hz, 1H). ESI-MS m/z (%) 261.1030 (100) $[M+1]^+$.

2.2.4. Synthesis of $[(dpio)_2Ir(\mu\text{-}Cl)]_2$

0.65 g (2.5 mmol) DPIO in 22.5 mL ethylene glycol ether and 0.35 g (1 mmol) $IrCl_3{\cdot}3H_2O$ in 7.5 mL water were added into a 100 mL round-bottom flask. The reaction solution was heated to reflux under nitrogen atmosphere for 24 hours. After the reaction was completed, the reaction solution was a dark purple turbidite solution. Cooled it to room temperature and the solvent was removed under rotary vacuum. The solid was collected by suction filtration and further washed by CH_2Cl_2, methanol and water in sequence to give $[(dpio)_2Ir(\mu\text{-}Cl)]_2$ as gray powder with a yield of 51.1 %.

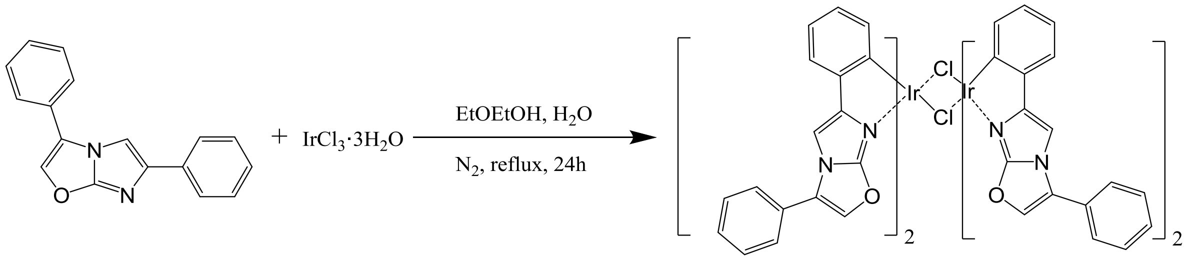

Scheme 3. Synthesis of $[(dpio)_2Ir(\mu\text{-}Cl)]_2$

2.2.5. General synthesis of Iridium(III) complexes

0.15 g (0.1 mmol) $[(dpio)_2Ir(\mu\text{-}Cl)]_2$, and 0.25 mmol of auxiliary ligand (0.04 g quinoline-2-carboxylic acid (2-QA), 0.04 g isoquinoline-3-formic acid (3-IQA), and 0.03 g 2-picolinate (pic), respectively) and 0.15 g (0.1 mmol) anhydrous sodium carbonate were added in 6 mL DMF in a 50 mL round bottom flask. The reaction mixture was heated to reflux under nitrogen atmosphere for 24 hours. After the reaction was completed, cooled to room temperature and DMF was removed. The residue was purified by column chromatography (CH_2Cl_2: methanol from 40:1 to 4:1, volume ratio) to obtain title complexes.

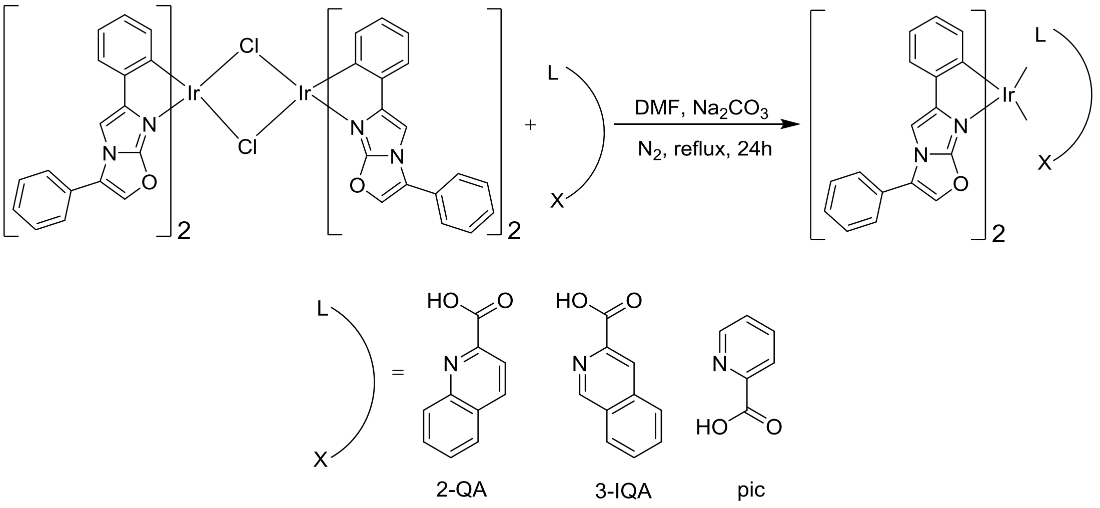

Scheme 4. Synthesis of iridium(III) complexes

(iridium(III)bis(3,6-diphenylimidazo[2,1-b]oxazole)(quinoline-2-carboxylic acid), (dpio)$_2$Ir(2-QA): red powder, yield: 60.6 %. ^{1}H NMR (500 MHz, DMSO) δ 8.65 (d, J = 8.5 Hz, 1H), 8.60 (s, 1H), 8.38 (s, 1H), 8.33 (d, J = 8.9 Hz, 1H), 8.31-8.24 (m, 2H), 8.14 (s, 1H), 8.04 (d, J = 8.0 Hz, 1H), 7.95 (s, 1H), 7.81 (d, J = 7.5 Hz, 2H), 7.77 (d, J = 7.5 Hz, 2H), 7.56 (t, J = 6.8 Hz, 4H), 7.51 (t, J = 7.2 Hz, 4H), 7.22 (t, J = 7.5 Hz, 1H), 6.83-6.74 (m, 2H), 6.66 (t, J = 7.2 Hz, 1H), 6.56 (t, J = 7.3 Hz, 1H), 6.49 (d, J = 7.6 Hz, 1H), 6.15 (d, J = 7.6 Hz, 1H). ^{13}C NMR (125 MHz, DMSO) δ 173.89, 162.79, 155.20, 154.14, 153.41, 148.31, 140.29, 139.44, 136.21, 135.77, 130.48, 130.27, 129.80, 129.44, 128.70, 127.42, 125.93, 125.08, 123.62, 121.45, 120.60, 102.78. ESI-MS m/z (%) 884.1917 (100) [M+1]$^+$.

(iridium(III)bis(3,6-diphenylimidazo[2,1-b]oxazole)(isoquinoline-3-carboxylic acid), (dpio)$_2$Ir(3-IQA): pale yellow powder, yield: 30.1 %. ^{1}H NMR (500 MHz, DMSO) δ 8.63 (2H, d, J = 7.5 Hz, H-6), 8.59 (1H, s, H-4’), 8.36 (4H, d, J = 10 Hz, H-2’”,6’”), 8.25 (1H, d, J = 8.0 Hz, H-5’), 8.22 (2H, s, H-4”), 7.96 (1H, d, J = 8.0 Hz, H-8’), 7.90 (1H, t, J = 8.0 Hz, H-7’), 7.84 (2H, d, J = 7.5 Hz, H-3), 7.77 (2H, t, J = 7.5 Hz, H-5), 7.73 (1H, t, J = 7.5 Hz, H-6’), 7.62 (2H, t, J = 8 Hz, H-4), 7.39 (2H, t, J = 8 Hz, H-4’”), 7.28 (1H, s, H-1’), 7.60-7.50 (5H, m, H-3’”, 5’”, 7’), 6.59 (1H, t, J = 7.5 Hz, H-6’), 6.43 (1H, d, J = 7.5 Hz, H-5’), 6.28 (1H, d, J = 7.5 Hz, H-8’), 5.44 (2H, s, H-1”). ^{13}C NMR (125 MHz, DMSO) δ 129.85, 129.77, 125.96, 125.76. ESI-MS m/z (%) 413.2385 (100) [M-(3-IQA)-(dpio)+23]$^+$.

(iridium(III)bis(3,6-diphenylimidazo[2,1-b]oxazole)(picolinic acid), (dpio)$_2$Ir(pic): pale yellow powder, yield: 57.8 %。^{1}H NMR (500 MHz, DMSO) δ 8.66 (s, 1H), 8.39 (s, 2H), 8.37 (s, 1H), 8.04 (d, J = 4.0 Hz, 2H), 7.97 (d, J = 5.1 Hz, 1H), 7.87 (d, J = 7.5 Hz, 2H), 7.83 (d, J = 7.5 Hz, 2H), 7.60 (s, 2H), 7.58 (s, 2H), 7.54 (d, J = 7.1 Hz, 2H), 7.50 (t, J = 7.6 Hz, 3H), 6.81-6.77 (m, 1H), 6.74 (d, J = 7.2 Hz, 1H), 6.63-6.54 (m, 2H), 6.35 (d, J = 7.6 Hz, 1H), 6.24 (d, J = 7.5 Hz, 1H). ^{13}C NMR (125 MHz, DMSO) δ 172.62, 147.95, 143.99, 139.09, 137.09, 134.50, 133.94, 132.39, 129.28, 127.93, 127.21, 125.57, 123.44, 103.80. ESI-MS m/z (%) 834.1685 (100) [M+1]$^+$.

3. Result and discussion

3.1. Photophysical properties

The UV-vis absorption spectra of the title complexes in DMF are shown in Fig. 1 and the related data are listed in Table 1. All complexes exhibit intense UV absorption bands attributable to the spin-allowed Ligand centered (^{3}LX) transitions at higher energies before 380 nm, while an admixture of metal-to-ligand charge transfer states (^{1}MLCT and ^{3}MLCT) appears at lower energies after 400 nm with lower extinction coefficients. These results indicate that there is a strong spin-orbit coupling between the singlet and triplet states of the title complexes, and their UV-vis absorption peaks are adjustable by changing the structure of the auxiliary ligands.

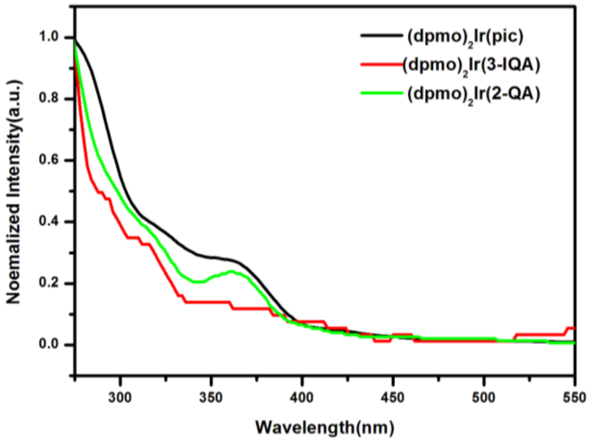

Fig. 1 The UV-vis spectra of iridium(III) complexes (color online)

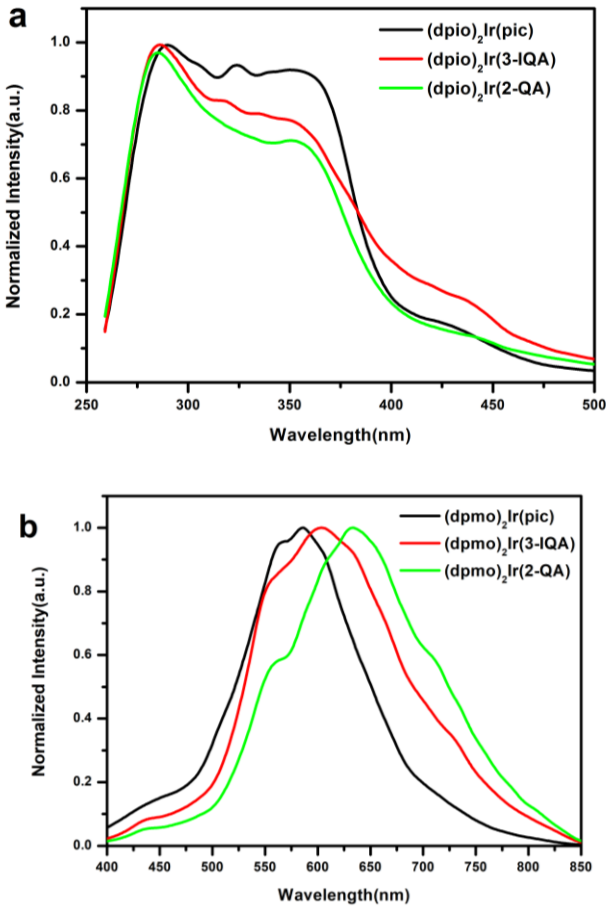

Fig. 2. The fluorescence (a) excitation and (b) emission spectra of iridium(III) complexes (color online)

Table 1. The luminous performance of iridium(III) complexes

Complexes	**Absorption (λ, nm)**	**Excitation (λ_{max}, nm)**	**Emission (λ_{max}, nm)**	**CIE (x, y)**	**Φ_{em} (%)**
(dpio)$_2$Ir(pic)	249/281/366	290, 320	585	(0.18, 0.17)	18.4
(dpio)$_2$Ir(3-IQA)	227/255/267	291, 316	606	(0.19, 0.19)	14.3
(dpio)$_2$Ir(2-QA)	222/247/268	290, 309	637	(0.20, 0.23)	23.8

The excitation and emission spectra of the title complexes are shown in Fig. 2 and the related data are listed in Table 1. Their emission peaks cover a large range from 585 nm to 637 nm. Compared with the emission peak of (dpio)$_2$Ir(pic), the emission peaks of (dpio)$_2$Ir(2-QA) and (dpio)$_2$Ir(3-IQA) are red-shifted 52 nm and 21 nm respectively, due to their stronger conjugations. In comparison with (mpmt)$_2$Ir(2-QA), (mpmt)$_2$Ir(3-IQA) and (mpmt)$_2$Ir(pic) with 3-methyl-6-phenylimidazo[2,1-b]thiazole (mpmt) as the primary ligand [16], the emission peaks of title complexes red shift from 18 nm to 55 nm, which is mainly leaded by replacing sulfur atom with oxygen atom at the nitrogen end of C^N primary ligands. The main reason is that the electron-withdrawing group on the C^N ligand reduces the energy of the LUMO, which leads to the reduction of HOMO-LUMO energy gap, thus causing the red shift of light emitting. The internal quantum efficiencies of the title complexes ranged from 14.3% to 23.8%, and (dpio)$_2$Ir(2-QA) exhibit the highest internal quantum efficieny, which may be caused by the stronger structural rigidity because of the introduction of 2-QA as auxiliary ligand, similar to the performance of (mpmt)$_2$Ir(2-QA) [16].

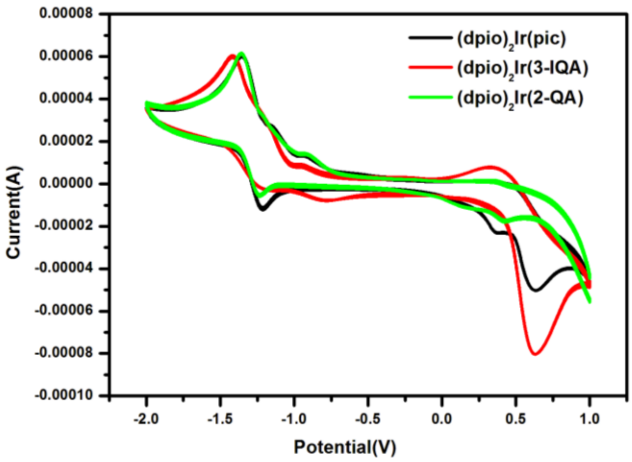

Fig. 3. The CV curves of iridium(III) complexes (color online)

3.2. Electrochemical properties

According to Equation 2, the HOMO energy levels of the title complexes were calculated by their initial oxidation potentials which were investigated by cyclic voltammetry experiment (CV, Fig. 3) at room temperature with ferrocene as a reference (4.8 eV). Further, their LUMO energy levels were calculated by the HOMO energy levels and the energy level gaps (E_g) which were estimated by the UV-vis absorption data.

$$\begin{aligned} HOMO &= -[E_{OX} - E_{Fc/Fc^+} + 4.8] \\ E_g &= 1240/\lambda \\ LUMO &= HOMO + E_g \end{aligned} \tag{2}$$

Table 2. The electrochemical data of iridium(III) complexes

Complexes	λ_{onest} (nm)	E_{ox} (eV)	HOMO (eV)	E_g (eV)	LUMO (eV)
$(dpio)_2Ir(pic)$	425	0.35	-4.73	2.92	-1.81
$(dpio)_2Ir(3\text{-}IQA)$	435	0.63	-5.01	2.87	-2.14
$(dpio)_2Ir(2\text{-}QA)$	475	0.43	-4.81	2.61	-2.2

As showing in Table 2, the oxidation peaks of title complexes are located from 0.35 eV to 0.63 eV, which is mainly caused by the ionic oxidation for Ir^{3+}/Ir^{4+} oxidation-reduction couple, and the oxidation potentials of $(dpio)_2Ir(3\text{-}IQA)$ are higher than these of $(dpio)_2Ir(2\text{-}QA)$ and $(dpio)_2Ir(pic)$, which may be the nitrogen substitutions at the 3-position of the quinoline more difficult to lose electron. In addition, it can be found that the energy level gaps (E_g) of $(dpio)_2Ir(2\text{-}QA)$ and $(dpio)_2Ir(3\text{-}IQA)$ are narrower than that of $(dpio)_2Ir(pic)$ due to their larger conjugation, which also lead to the fact that their emission peaks redshift from yellow to standard red light region .

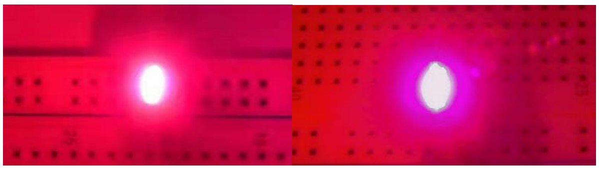

dpio)$_2$Ir(3-IQA) (dpio)$_2$Ir(2-QA)

Fig. 4. The light-emitting images of LEDs prepared with title complexes as light-emitting materials (color online)

3.3. Fabrication and performance of LEDs

In order to investigate the application potential of $(dpio)_2Ir(2\text{-}QA)$ and $(dpio)_2Ir(3\text{-}IQA)$ as standard red light emitting materials, LEDs basing on them were fabricated as follow procedures: The InGaN chip was glued to the bracket with a mold adhesive and baked in the oven at 150℃ for 1 hour. The adhesive was baked to make the chip and bracket to be sticked together. The positive and negative terminals of the chip are respectively connected to the positive and negative terminals of the bracket by gold wires. The glue and the solid powder of $(dpio)_2Ir(2\text{-}QA)$ or $(dpio)_2Ir(3\text{-}IQA)$ were mixed in 10:1 as weight ratio, and then added into the bracket cup that had been welded with the gold wire. Then the devices was put into the oven and cured at 150℃ for 1 hour. Epoxy resin is used to encapsulate the cured solder wire and powder semi-finished products. Epoxy resin is fully cured by heating aging; the whole piece of the holder is cut into single material, and the photoelectric parameters were tested under the excitation light source of 395 nm. Both of the LEDs exhibit standard red light emitting (as shown in Fig. 4), as the same as the corresponding liquid fluorescent emission spectra exhibition.

4. Conclusion

In this paper, 3, 6-diphenylimidazo[2,1-b]oxazole (dpio) has been synthesized in a convenient and environment friendly method, and three novel Ir^{III} complexes using it as primary ligand have been prepared and characterized. The results of related photophysical and electrochemical measurements show that the emission peaks of these complexes are from 585 nm to 637 nm, located in the yellow and red light region, and the quantum efficiency of light is between 14.3% and 23.8%. Among them, the complex $(dpio)_2Ir(2\text{-}QA)$ has the highest emission efficiency and is located in the standard red light region due to its larger conjugation degree.

Acknowledgments

We gratefully acknowledge the financial support of NSFC (No. 21461030), the Applied Basic Research Projects of Yunnan Province (No. 202101AT070217) and the Doctoral Scientific Research Foundation of Yunnan Normal University (No. 2019XJLK11).

References

[1] S. Hirata, Y. Sakai, K. Masui Shuzo Hirata, Yumi Sakai, Kensuke Masui, H. Tanaka, S. Y. Lee, H. Nomura, N. Nakamura, M. Yasumatsu, H. Nakanotani, Q. Zhang, K. Shizu, H. Miyazaki, C. Adachi, Nat. Mater. **14**(3), 330 (2015).

[2] M. Klessinger, Angew. Chem. Int. Ed. **34**(5), 49, 549(1995).

[3] C. Adachi, M. A. Baldo, S. R. Forrest, M. E. Thompson, Appl. Phys. Lett. **7**(6), 904 (2000).

[4] R. Bujaldon, N. Peinka, M. Reig, A. Cuadrado, C. Fabregat, M. Font-Bardia, E. Martinez-Ferrero Do Velasco, Opt. Mater. **111**, 110696 (2021).

[5] Z. Li, Z. Ge, X. Tong, L. Guo, J. Huo, D. Li, H. Li, A. Lu, T. Li, Dyes Pigm. **186**, 109016 (2021).

[6] H.-F. Li, X. Q. Liu, C. Lyu, J. Gorbaciov, L.-L. Wen, G.-G. Shan, P. B. Wyatt, H.-Q. Ye, W. P. Gillin, Light Sci. Appl. **9**, 32 (2020).

[7] L. Y. Hsu, D. G. Chen, S. H. Liu, T.-Y. Chiu, C.-H. Chang, A. K.-Y. Jen, P.-T. Chou, Yun Chi, ACS Appl. Mater. Inter. **12**, 1084 (2020).

[8] Q. -M. Guo, G. -L Huang, X. -Y. Yin, J.-J. Bian, X.-M. Li, M.-Y. Teng, Bull. Korean Chem. Soc. **41**, 1184 (202).

[9] Y. Wan, Y. P. Xiao, Y. Y. Zhou, C.-G. Hu, B.-H. Tong, S.-H. Ye, Q.-B. Mei, Dalton Trans. **48**, 16289 (2019).

[10] H. -T. Mao, Y. Cui, G. -F. Li, G.-G. Shan, Q.-Y. Zeng, F.-S. Li, Z.-M. Su, J. Mater. Chem. C **7**, 13461 (2019).

[11] L. Y. Hsu, Q. Liang, Z. Wang, H.-H. Kuo, W.-S. Tai, S.-J. Su, X. Zhou, Y. Yuan, Y. Chi, Chem. Eur. J. **25**, 15375 (2019).

[12] L. Zhang, Z. -P. Yan, Z. -L. Tu, Z.-G. Wu, Y.-X. Zheng, J. Mater. Chem. C **7**, 11606 (2019).

[13] C. You, D. Liu, F. Meng, Y. Wang, J. Yu, S. Wang, S. Su, W. Zhu, J. Mater. Chem. C **7**, 10961 (2019).

[14] Y. -K. Chen, H. -H. Kuo, D. Luo, Y.-N. Lai, W.-C. Li, C.-H. Chang, D. Escudero, A. K.-Y. Jen, L.-Y. Hsu, Y. Chi, Chem. Mater. **31**, 6453 (2019).

[15] M. Luo, A. Liang, Z. Wang, H. Wang, T. Cao, D. Liu, Y. Chen, D. Ma, Opt. Mater. **91**, 439 (2019).

[16] X. -Y. Yin, Z. -Y. Yang, G. -L. Huang, J.-J. Bian, D.-Q. Wang, Q. Wang, M.-Y Teng, Z.-L. Wang, J. Zhang, New J. Chem. **43**, 5849 (2019).

[17] K. A. King, P. J. Spellane, R. J. Watts. J. Am. Chem. Soc. **107**, 1431 (1985).

[18] P. Sebastian, M. Tulodzoecki, M. P. Bernicola, V. C. E. Gomez, Y. Shao-Horn, J. M. Feliu, ACS Appl. Energ. Mater. **1**, 4617 (2018).

---

[*] Corresponding authors: myteng@ynnu.edu.cn;
wqin@foxmail.com;
boboo2558@163.com;